national accelerator laboratory

NAL-Pub-74/18-EXP
2257.000

Yale 3075-65

(Submitted to Phys. Rev. Letters)

$|g_A/g_V|$ IN THE DECAY $\Sigma^- \rightarrow ne^-\bar{\nu}$

W. Tanenbaum, V. Hungerbuehler, R. Majka, J. Marx,
P. Némethy, J. Sandweiss, and W. Willis
Yale University, New Haven, Connecticut 06520 USA

M. Atac, S. Ecklund, P. J. Gollon, J. Lach, J. MacLachlan,
A. Roberts, R. Stefanski, and D. Theriot
National Accelerator Laboratory, Batavia, Illinois 60510 USA

and

C. L. Wang
Brookhaven National Laboratory, Upton, New York 11973 USA

January 1974

NAL-Pub-74/18-EXP
Yale 3075-65

$|g_A/g_V|$ IN THE DECAY $\Sigma^- \rightarrow ne^-\bar{\nu}$

W. Tanenbaum, V. Hungerbuehler,[*] R. Majka, J. Marx, P. Némethy, J. Sandweiss, and W. Willis[†]
Yale University, New Haven, Connecticut 06520 USA[‡]

M. Atac, S. Ecklund, P. J. Gollon, J. Lach, J. MacLachlan, A. Roberts, R. Stefanski, and D. Theriot
National Accelerator Laboratory, Batavia, Illinois 60510 USA[**]

and

C. L. Wang
Brookhaven National Laboratory, Upton, New York 11973 USA[††]

ABSTRACT

The decay $\Sigma^- \rightarrow ne^-\bar{\nu}$ was studied using the Yale-NAL-BNL hyperon beam at the Brookhaven AGS. The Σ^- and e^- momenta were measured by magnetic spectrometers with magnetostrictive wire spark chambers. A threshold Cerenkov counter and a total absorption calorimeter identified the electron and neutron respectively. From a sample of 3507 reconstructed events we have found $|g_A/g_V| = 0.435 \pm 0.035$.

We report a measurement of the magnitude of the ratio of the axial vector to vector form factors, $|g_A/g_V|$, from the observation of 3507 decays of the type $\Sigma^- \rightarrow ne^-\bar{\nu}$. These events were produced using the Yale-NAL-BNL high-energy negative hyperon beam at the Brookhaven National Laboratory (BNL) Alternate Gradient Synchrotron (AGS).[1] The hyperon beam delivers a flux of approximately 200 Σ^- per machine pulse produced in the forward direction at a central momentum of 23 GeV/c at the exit of the magnetic channel. Figure 1 depicts the beam and the associated electronic detection apparatus which are described in more detail elsewhere.[1] Beam particles of mass less than that of a proton are vetoed by a threshold Cerenkov counter (C_B) which forms part of the beam channel and also vetoed by a scintillation counter (V_π) located at the downstream end of the apparatus. A set of small counters (B) and a hole veto counter (V_H) define the beam and discriminate against upstream hyperon decays. A cluster of high pressure, high resolution magnetostrictive spark chambers[2] determine the momentum of the emerging hyperons to 1%.

Located downstream of the 115-in. decay region is a magnetic spectrometer with conventional magnetostrictive wire spark chambers which determines the momentum of the electron from the decay $\Sigma^- \rightarrow ne^-\bar{\nu}$ to about 5%. Situated after the spectrometer is a Cerenkov counter ($\check{C}$) filled with hydrogen at atmospheric pressure. This counter, which has a large phase space acceptance, identifies electrons from the desired leptonic decay among the more copious pions produced in the major decay mode, $\Sigma^- \rightarrow n\pi^-$. This counter suppresses the trigger rate for the major decay mode by a factor of approximately 80. Following the Cerenkov counter is a hodoscope of scintillation counters (S), each of which shadows one of the five optical cells of the electron Cerenkov counter. In addition, the counter nearest to the beam line is backed by a lead and scintillator shower counter to give extra discrimination against nonleptonic backgrounds.

A neutron detector[3] is located at the end of the apparatus, following a second spectrometer magnet which is used to study other hyperon decays not reported here. It consists of a set of 5 modules, each having a 1.25 in. iron plate, an XY multiwire proportional chamber with 1-cm wire spacing, and a scintillation counter. It is followed by an iron-scintillator hadron calorimeter. The interaction point of the decay neutron is determined from the spatial distribution of the resulting hadron shower in the five modules. By use of a complex algorithm[4] the neutron interaction point can be determined to better than 1 cm (rms) for 85% of the events. As a result the direction of the decay neutron is determined to better than 1 mrad. The hadron calorimeter (NC) is used to discriminate against background muons by requiring a minimum pulse height in the trigger. The crude information on the neutron energy (±25%) is not used in the reconstruction.

The decay $\Sigma^- \rightarrow ne^-\bar{\nu}$ was signified by the trigger

$$\bar{C}_B \cdot B \cdot \bar{V}_H \cdot \check{C} \cdot S \cdot NC \cdot \bar{V}_\pi.$$

Two-body decays, $\Sigma^- \rightarrow n\pi^-$, and beam pions were also recorded at a scaled down rate to provide a flux normalization and to monitor the efficiency and resolution of the chambers and neutron detector. The total trigger rate was a few per machine pulse. For each trigger we recorded the configuration of scintillation counter hits, the pulse heights from the electron Cerenkov counter, shower counter and hadron calorimeter, the time difference between signals from the electron Cerenkov counter and the S counter hodoscope as well as the spark chamber and multiwire proportional chamber information. The major source of background in the leptonic trigger came from the decay $\Sigma^- \rightarrow n\pi^-$ in time with a background muon which triggered the electron Cerenkov counter. A major task of the analysis was to remove this background (which is thrice overconstrained) from the signal of leptonic decays.

The first stage of the analysis was to require of all potential leptonic events a beam track which could be extrapolated to the hyperon production target within the beam channel phase space, a well-defined negative track in the spectrometer making an angle greater than 9 mrad with the beam track, and a reconstructed decay vertex in the decay fiducial region. Figure 2(a) shows the beam mass spectrum of events passing these criteria when reconstructed under the $\Sigma^- \rightarrow n\pi^-$ hypothesis. The broad distribution contains the leptonic events and the sharp peak at the Σ^- mass the two-body background. A reduction of the nonleptonic background was made by requiring a large pulse height in the shower counter when relevant, a proper time difference between the electron Cerenkov counter and appropriate S counter, and by requiring that the reconstructed negative track point to the proper cell of the Cerenkov counter and the proper S counter. These consistency requirements serve to define decay electrons and eliminate events having a background muon triggering the electron Cerenkov counter, reducing the nonleptonic backgrounds to the level depicted in Fig. 2(b). The final sample of 3507 $\Sigma^- \rightarrow ne^-\bar{\nu}$ decays results from a cut requiring the reconstructed Σ^- mass, assuming the hypothesis $\Sigma^- \rightarrow n\pi^-$, to be less than 1165 MeV.

Since for this leptonic decay there is a square root ambiguity resulting from the zero constraint fit, we cannot assign an event a unique position on a Dalitz plot. In order to obtain the maximum information in a bias free manner, both solutions were kept and each event plotted on a three-dimensional Dalitz plot. The electron energy and two neutron energies define the coordinates. The form factor ratios were obtained from the final event sample by a maximum likelihood fit to projections of the three-dimensional "Dalitz plot" weighted by a Monte Carlo calculation of the acceptance of the detection apparatus. Our center-of-mass neutron and electron energy resolution (about 5 MeV) corresponds to 5 neutron energy bins for each solution and 20 electron energy bins.

Data were taken for two values of the magnetic field in the spectrometer magnet. This had the advantage of giving two data samples with different amounts of nonleptonic backgrounds and different detection efficiencies. The two results for the absolute value of the form factor ratio as computed from a likelihood function ($\mathcal{L}$) fit to the neutron spectrum only are presented in Table I. In obtaining these results, it was assumed that second-class currents are negligible and that the effect of weak magnetism is that predicted by the Conserved Vector Current hypothesis (CVC). The result is quite insensitive to the amount of weak magnetism present.

In order to evaluate the quality of the likelihood fit of the data to the usual parametrization of the weakly interacting hadronic current, Monte Carlo techniques were used to generate a number of event samples of equivalent statistics to the data sample. The measured form factor ratios were used as inputs to the Monte Carlo program which included the effects of experimental resolution. These events were then analyzed in a manner identical to that used for the data. A comparison between the value of the likelihood fits for the data and Monte Carlo generated event samples is also presented in Table I.

The errors assigned to $|g_A/g_V|$ are purely statistical. However, none of the small systematic corrections considered contributes significant uncertainties. The final result for the absolute value of the form factor ratio is obtained by averaging the results from the two data samples to yield:

$$|g_A/g_V| = 0.435 \pm 0.035.$$

It is interesting to note that the Cabibbo theory[5] predicts $g_A/g_V = 0.33 \pm 0.04$. Table II contains a comparison of this experiment with the results of previous experiments.

We wish to thank our engineering staff, Andy Disco, Satish Dhawan, Cordon Kerns, Stan Lasinski, Blaise Lombardi and Irving Winters, and our technicians Alan Wandersee, Jon Blomquist and Ed Steigmeyer for their help in the design and setup of the apparatus. We also thank the AGS staff, in particular, David Berley, Eugene Halek and Gerry Tanguay for providing the technical support needed for the success of this experiment.

REFERENCES

[*] Present address: Universite de Geneve, Geneve, Switzerland

[†] Present address: CERN, Geneva, Switzerland

[‡] Research supported by the United States Atomic Energy Commission under Contract AT(11-1).

[**] Operated by Universities Research Association Inc. under contract with the United States Atomic Energy Commission.

[††] Supported in part by the United States Atomic Energy Commission.

[1] V. Hungerbuehler et al., The Design and Operation of the Yale-NAL-BNL Hyperon Beam, National Accelerator Laboratory Report NAL-Pub-73/53-EXP and Yale-3075-49, August 1973, to be published in Nucl. Instr. and Methods.

[2] W. J. Willis et al., Nucl. Instr. and Methods 91, 33 (1971).

[3] M. Atac et al., Nucl. Instr. and Methods 106, 263 (1973).

[4] W. Tanenbaum, Nucl. Instr. and Methods 106, 269 (1973).

[5] H. Ebenhöh et al., Z. Physik 241, 473 (1971).

[6] A. P. Colleraine et al., Phys. Rev. Letters 23, 198 (1969).

[7] F. Eisele et al., Z. Physik 223, 487 (1969).

[8] C. Baltay et al., Phys. Rev. D5, 1569 (1972).

Table I. Results for $|g_A/g_V|$ and Maximum Value of Likelihood Fits From Neutron Spectrum in c.m.

Spectrometer Field Integral	6 kG-m	13 kG-m
$\|g_A/g_V\|$	0.420±0.045	0.455±0.055
$\ln \mathcal{L}$ (data)	-51.68	-52.11
$\ln \mathcal{L}$ (Monte Carlo)	-53.28±3.26	-49.62±3.18
Probability $\mathcal{L}$(Monte Carlo) $<\mathcal{L}$(data)	69%	22%

Table II. Summary of $\Sigma^- \rightarrow ne^- \bar{\nu}$ Form Factor Experiments.

Experiment	Year	No. of Events	$\|g_A/g_V\|$
Maryland[6]	1969	49	0.23±0.16
Heidelberg[7]	1969	33	$0.37^{+0.26}_{-0.19}$
Columbia-Stony Brook[8]	1972	36	$0.29^{+0.28}_{-0.29}$
This Experiment	1973	3507	0.435±0.035

FIGURE CAPTIONS

Fig. 1. Schematic diagram of the high-energy hyperon beam at the BNL AGS.

Fig. 2(a). Mass spectrum of beam particles for leptonic decays at an early stage of the analysis when reconstructed under the $\Sigma^- \to n\pi^-$ hypothesis. The leptonic events being sought are in the broad tail, the two-body background events are in the sharp peak.

Fig. 2(b). The same spectrum at the last stage in the analysis. A final mass cut of 1165 MeV was made and events below that mass were considered to be leptonic decays.

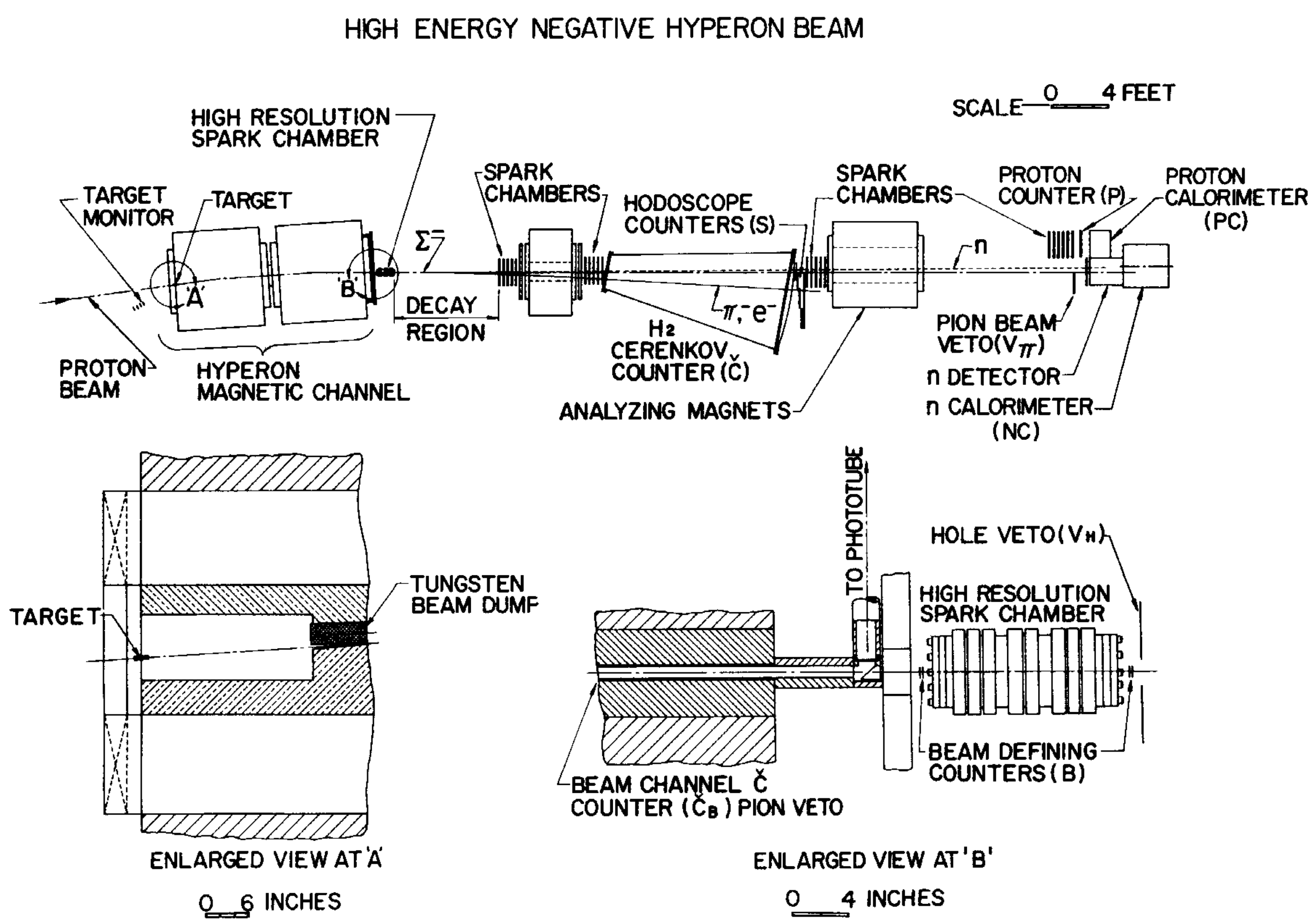
HIGH ENERGY NEGATIVE HYPERON BEAM
SCALE 0 4 FEET
HIGH RESOLUTION SPARK CHAMBER
TARGET MONITOR
TARGET
A
B
Σ⁻
SPARK CHAMBERS
HODOSCOPE COUNTERS (S)
SPARK CHAMBERS
PROTON COUNTER (P)
PROTON CALORIMETER (PC)
n
DECAY REGION
π⁻, e⁻
PROTON BEAM
HYPERON MAGNETIC CHANNEL
H₂ CERENKOV COUNTER (Č)
ANALYZING MAGNETS
PION BEAM VETO(Vπ)
n DETECTOR
n CALORIMETER (NC)
TARGET
TUNGSTEN BEAM DUMF
TO PHOTOTUBE
HOLE VETO(VH)
HIGH RESOLUTION SPARK CHAMBER
BEAM DEFINING COUNTERS (B)
BEAM CHANNEL Č COUNTER (ČB) PION VETO
ENLARGED VIEW AT 'A'
0 6 INCHES
ENLARGED VIEW AT 'B'
0 4 INCHES

Fig. 1

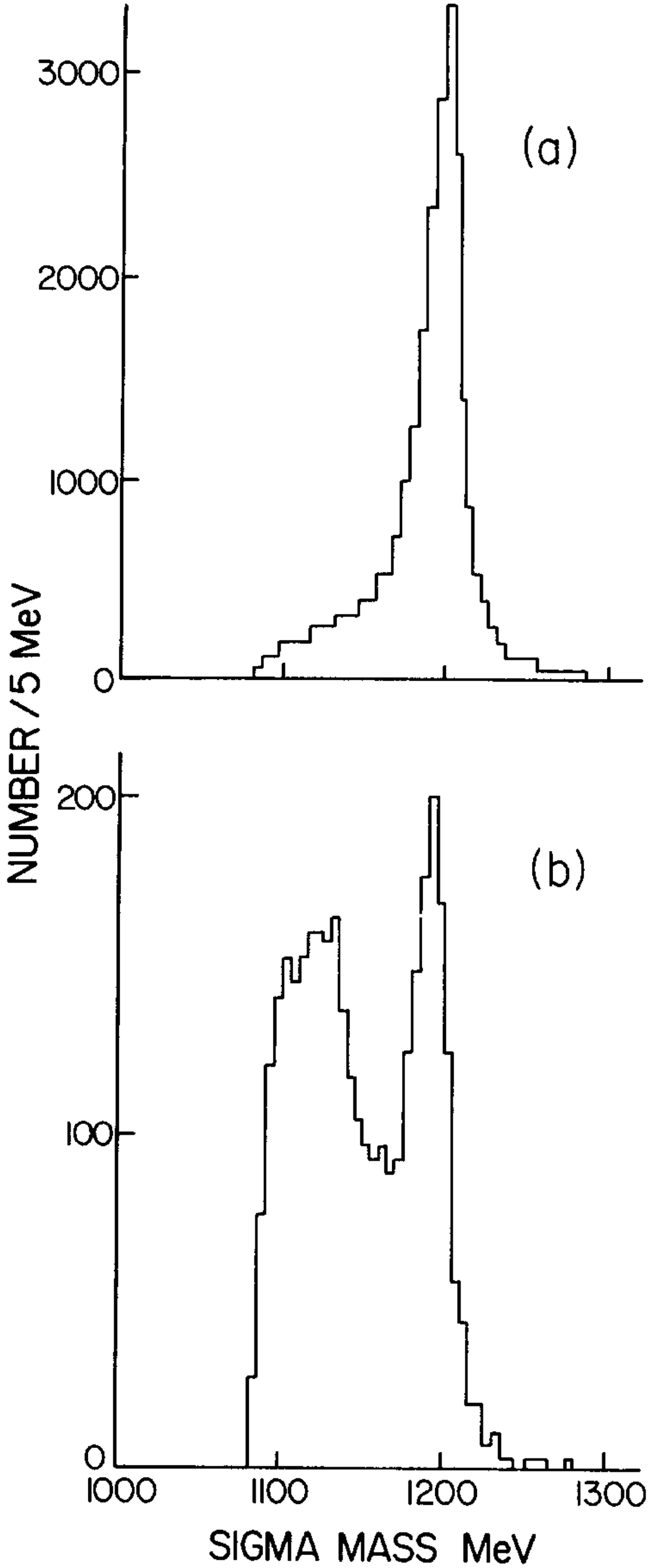

3000
2000
1000
0
(a)
NUMBER /5 MeV
200
100
0
(b)
1000
1100
1200
1300
SIGMA MASS MeV

Fig. 2